ACS SyntheticBiology

Letter

pubs.acs.org/synthbio

Manipulation of Endogenous Kinase Activity in Living Cells Using Photoswitchable Inhibitory Peptides

Jason J. Yi,[†,‡,#] Hui Wang,[†,#] Marco Vilela,[§] Gaudenz Danuser,[§] and Klaus M. Hahn*[,†]

[†]Department of Pharmacology and [‡]Department of Cell Biology and Physiology, University of North Carolina at Chapel Hill, Chapel Hill, North Carolina 27599, United States

[§]Department of Cell Biology, Harvard Medical School, Boston, Massachusetts 02115, United States

Supporting Information

ABSTRACT: Optogenetic control of endogenous signaling can be an important tool for probing cell behavior. Using the photoresponse of the LOV2 domain of *Avena sativa* phototropin 1, we developed analogues of kinase inhibitors whose activity is light dependent. Inhibitory peptides were appended to the Jα helix, where they potently inhibited kinases in the light but were sterically blocked from kinase interaction in the dark. Photoactivatable inhibitors for cyclic-AMP dependent kinase (PKA) and myosin light chain kinase (MLCK) are described, together with studies that shed light on proper positioning of the peptides in the LOV domain. These inhibitors altered endogenous signaling in living cells and produced light-dependent changes in cell morphodynamics.

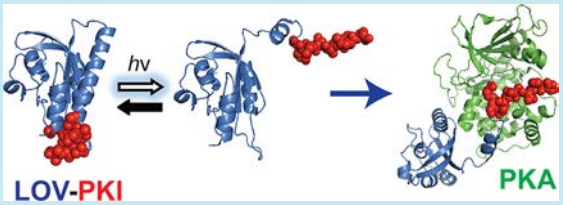

KEYWORDS: *optogenetics, peptide caging, PKA, MLCK, CREB, membrane dynamics*

Protein phosphorylation is a ubiquitous and essential mechanism of cell regulation and plays important roles in pathology.[1] This reaction is catalyzed by a large superfamily of kinases, which accounts for nearly 2% of the genes in the human genome.[2,3] Studying kinase function using genetic manipulation or small-molecule pharmacological agents provides poor spatial and/or temporal resolution, limiting our ability to examine how subcellular localization and the kinetics of protein phosphorylation contribute to regulation. New molecular tools are needed to probe the role of kinases in native cellular environments.

There has been considerable progress in developing genetically encoded, light-controlled molecules that can manipulate biological processes in living cells and animals. Many of these applications utilize analogues of proteins, where the protein of interest has been fused to light-responsive protein domains, or to proteins that interact with such domains (reviewed in the literature[4]). This can affect the normal biological activity of the target protein and is typically implemented through overexpression of ectopic proteins. Recently, the light-sensitive LOV2 domain from *Avena sativa* phototropin 1 (here referred to as LOV2) was adapted to control the activity of peptides.[5,6] We extend this work to control peptides that inhibit kinases and demonstrate that the approach can control endogenous kinases in living cells.

LOV2 is a member of the PAS superfamily.[7] It contains a flavin mononucleotide (FMN) cofactor located in the center of the PAS fold and a large α-helical region at the C-terminus of the fold termed the Jα helix.[8,9] Upon exposure to blue light, a covalent adduct is formed between the FMN and a cysteine side chain in the PAS fold, leading to a large conformational change that ultimately causes the unfolding of the Jα helix (Figure 1A).[7,10−12] When irradiation ceases, reversion of the thiol bond and a conformational change back to the dark state occurs.[13] We hypothesized that these conformational changes could be used to control inhibitory peptides with light, providing a selective and minimally invasive way to manipulate endogenous signaling pathways *in vivo*.

We began our study by choosing regions within the LOV2 sequence that could serve as sites for peptide incorporation, where light-induced conformational changes might affect exposure of the peptide. We first selected the flexible loop between the PAS fold of LOV2 and the Jα helix (Figure 1B). For our initial studies, we selected the widely used naturally occurring PKA inhibitory peptide PKI. The PKI gene encodes a heat-stable, 76-amino acid peptide that acts as a high-affinity, highly selective competitive inhibitor of the catalytic subunit of PKA (K_i 2.5−36 nM).[14] The pseudosubstrate region of PKI is between amino acids 18−22, and PKI is commonly used as a 17-amino acid fragment encompassing amino acids 6−22 (PKI 6−22), or as a shorter 9-amino acid fragment encompassing amino acids 14−22 (PKI 14−22). Moreover, the expression of PKI fusion proteins has been shown to effectively dampen PKA signaling in living cells.[15,16] We incorporated the shorter PKI 14−22 between the Thr517 and Glu518 residues of the LOV2 sequence along with flanking Gly-Ser linkers to retain peptide flexibility (PKI 14−22 Int; Figure 1B). We expressed a "dark state" mutant (C450A) of LOV2 that abolishes FMN-thiol bond formation,[17] or a "lit state" mutant (I539E) that

Special Issue: Synthetic Photobiology

Received: March 7, 2014
Published: June 6, 2014

   dx.doi.org/10.1021/sb5001356 | *ACS Synth. Biol.* 2014, 3, 788−795

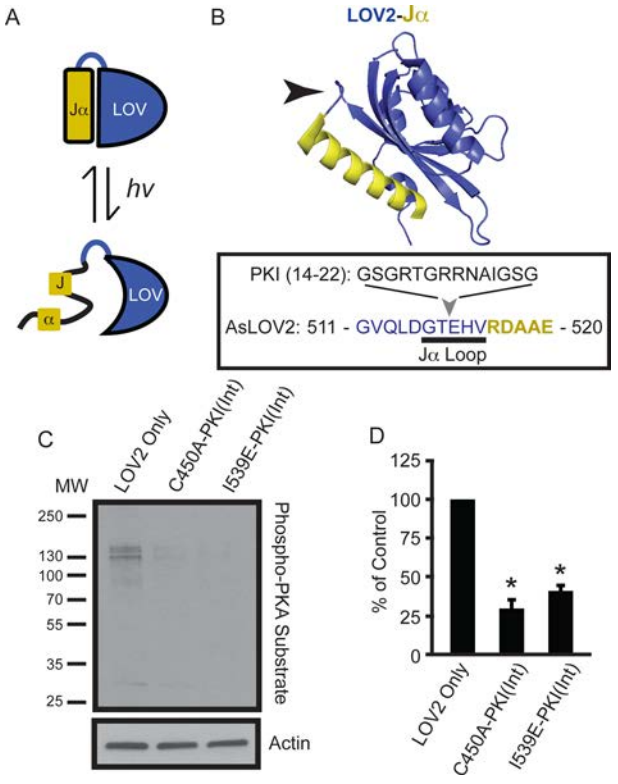

Figure 1. Perturbation of dark-state LOV2 due to peptide incorporation in the Jα loop. (A) Schematic showing the light response of LOV2. Blue represents the LOV2 globular domain, yellow represents the Jα helix. Upon irradiation with blue light, a conformational change in LOV2 causes the unwinding of Jα. (B) Crystal structure of LOV2 showing the PAS fold of LOV2 (blue), the Jα helix (yellow), and the loop region connecting the two domains (arrowhead). The sequence of PKI and its incorporation between Thr517 and Glu518 are shown in the box. (C) Western blot showing total phosphorylated PKA substrates in HEK293 cells and actin loading control. Note the loss of PKA phosphorylation in both dark-state mutant (C450A) and light-state mutants (I539E). (D) Quantification of (C), $n = 4$, $^*p < 0.01$, Student's t test.

destabilizes the Jα helix[10] in HEK293 cells. PKA activity was stimulated using the adenylyl cyclase agonist forskolin (10 μM, 1.5 h), and PKA activity monitored by Western blot using an antibody that specifically recognizes phosphorylated PKA motifs.[18] We found that both C450A and I539E mutants were able to inhibit PKA activity (Figure 1C,D; C450A, 29.6 ± 5.9%; I539E, 41.2 ± 4.5% compared to LOV2 alone). As it was unlikely that the peptide could adopt a PKA-interacting conformation in both the lit and dark state structures, this data suggested that peptide incorporation at this site altered the folding of LOV2. In a previous study, our laboratory created a photoswitchable version of the Rac GTPase using LOV2 (PA-Rac).[19] By incorporating the PKI sequence into this construct at the loop position described above (between Thr517 and Glu518), we could test whether peptide incorporation affected light-induced conformational changes. Light-dependence of Rac activity was examined using a previously established biochemical method for assessing Rac activation, in which Rac was pulled down with the CRIB domain of the Rac effector p-21 activated kinase (Figure S1B, Supporting Information).[20] Indeed, pulldown of wild-type PA-Rac increased with light, but the light response was lost with loop incorporation of PKI (Figure S1, Supporting Information).

On the basis of our previous studies of peptide interactions with the Jα helix,[5,6] we next examined whether we could cage PKI by embedding it in the C-terminus of this helix. The three-dimensional structure of LOV2-PKI C-terminal fusions were modeled using the I-TASSER algorithm.[21,22] Intriguingly, whereas PKI 6−22 became unstructured at its C-terminal end, PKI 14−22 remained helical within the Jα helix, suggesting that the length of the peptide sequence may predominantly determine the success of C-terminal peptide incorporation (Figure 2A−C). Experiments were consistent with this

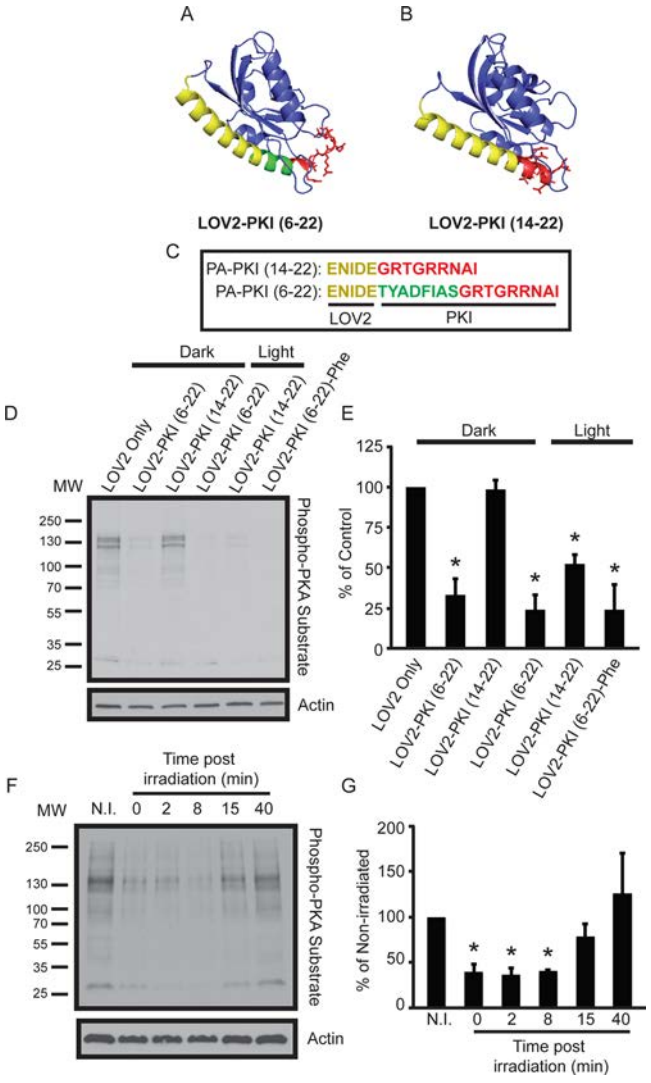

Figure 2. Photoswitchable response of LOV2-PKI 14−22. (A) I-TASSER prediction of the structure of LOV2-PKI 6−22 and LOV2-PKI 14−22 (B). The Jα helix (yellow), the PKI 14−22 sequence (red), and the variable linker region of PKI 6−22 (green) are indicated. (C) Sequence showing the C-terminal fusion of PKI to LOV2. Amino acids 537−541 are shown for LOV2 in yellow. Green represents the variable PKI sequence and red the core PKI inhibitory region. (D) Western blot showing the dark and light response of LOV2-PKI 6−22 and LOV2-PKI 14−22, LOV2-PKI 6−22Phe, and actin loading control. Note the inhibition of phosphorylation in LOV2-PKI 14−22 only upon irradiation. LOV2-PKI 6−22Phe is shown in the dark. (E) Quantification of (D), $n = 4$, $^*p < 0.01$, Student's t test. (F) Western blot showing the recovery of PKA signaling upon cessation of light stimulation. (G) Quantification of (F), $n = 4$, $^*p < 0.01$, Student's t test.

dx.doi.org/10.1021/sb5001356 | ACS Synth. Biol. 2014, 3, 788−795

prediction: LOV2-PKI 6−22 inhibited induction of PKA signaling in both the light and the dark (Figure 2D,E; Dark, 33.3 ± 14.2% of control; Light, 24.1 ± 12.0% of control), but for cells expressing LOV2-PKI 14−22, PKA induction was substantially reduced in the light but not in the dark (Figure 2D,E; Dark, 98.4 ± 5.1% of control; Light, 52.5 ± 14.6%). In previous work we described an interaction between a C-terminal phenylalanine and a hydrophobic patch within LOV2 that could enhance light dependent caging of C terminal peptides on LOV.[5] However, this failed to have an effect here (LOV2-PKI 6−22Phe, Figure 2D,E; 24.0 ± 19.8% of control).

We found that the C-terminal fusion of PKI inhibited PKA signaling to a similar degree as cell-permeable PKI peptide (Figure S2, Supporting Information). Moreover, in reversibility assays, we found that PKA activity returned to basal states between 15−40 min after the cessation of blue light (Figure 2F,G; 0 min, 39.8 ± 7.8%; 2 min, 36.1 ± 9.9%; 8 min, 40.4 ± 6.1%; 15 min, 78.6 ± 15.0%; 40 min, 126.1 ± 27.4%). These results demonstrate that the C-terminal fusion of PKI could effectively inhibit PKA signaling in the presence of blue light in a reversible manner.

We renamed the LOV2-PKI 14−22 construct photoactivatable PKI (PA−PKI) and performed a set of experiments to determine its utility in living cells. In order to test the response of PA−PKI to light, we followed PKA-dependent phosphorylation of a single PKA substrate. We irradiated cells with blue light using a 460 nm LED array and monitored forskolin-dependent phosphorylation of cAMP response element-binding protein (CREB). CREB is a transcription factor that is activated through phosphorylation at Ser133 by an ensemble of kinases including PKA, protein kinase C (PKC), Ca^{2+}/calmodulin-dependent kinase (CaMK), p90Rsk, and MAPKAPK-2[23−28] (Figure 3A). We saw no effect on CREB induction using PA−PKI C450A in the light or PA−PKI WT in the dark (Figure 3B,C; C450A Light, 101.6 ± 1.7%; WT Dark, 98.7 ± 7.8% of control). In contrast, PA−PKI in the light produced a substantial reduction in forskolin-induced PKA phosphorylation that was comparable to that produced by existing reagents in previously published reports[29−32] (46.8 ± 10.4% of control; see Figure S2, Supporting Information, for comparison).

An important advantage of PA−PKI is its ability to affect PKA signaling in a subset of cells within a population. Primary cultured mouse cortical neurons aged 6 days *in vitro* (DIV 6) were sparsely transfected with PA−PKI or PA−PKI C450A for 48 h and stimulated with forskolin in the presence of blue light. Whereas a robust signal for phosphorylated PKA substrates was seen in the majority of cells, neurons expressing PA−PKI, but not PA−PKI C450A, showed a substantial decrease in PKA activity (Figure 4). When quantified, irradiation of cells expressing PA−PKI diminished PKA phosphorylation by ∼47% (Figure 4B; fluorescence intensity, C450A, 725.8 ± 48.07; WT, 390.9 ± 24.63). Together, these results demonstrate the ability of PA−PKI to target endogenous signaling events in living cells in a light-dependent manner.

We next asked if we could apply our methods to create additional photoswitchable inhibitory peptides. To this end, we selected myosin light chain kinase inhibitor peptide 18 (MKI).[33] Like CREB, myosin light chain 2, also known as myosin regulatory light chain, is targeted for phosphorylation by multiple kinases. These include myosin light chain kinase,[34] Rho kinase,[35] and the cell cycle regulator Cdc2[36] (Figure 5A). We employed a design similar to that used for PA−PKI, fusing

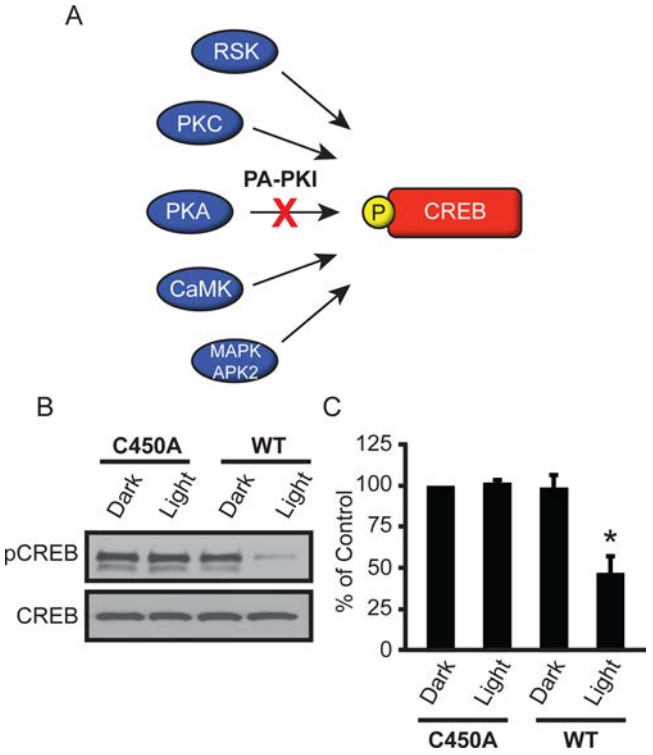

Figure 3. Light-dependent inhibition of CREB phosphorylation by PA−PKI. (A) Schematic showing pathway-dependent specificity of PA−PKI in CREB phosphorylation. (B) Loss of phosphorylated CREB (pCREB) but not total CREB upon irradiation in HEK293 cells. (C) Quantification of (B), $n = 3$, $^*p < 0.01$, Student's t test.

MKI to the C-terminus of Jα with a single glycine linker. I-TASSER modeling of this sequence showed that MKI adopted a helical conformation similar to PA−PKI (Figure 5B). When tested in HEK293 cells, we saw a dramatic light-dependent decrease in cellular levels of phosphorylated myosin light chain (Figure 5C,D). Phosphorylated myosin light chain levels were unaffected in irradiated cells expressing PA-MKI C450A and in nonirradiated cells expressing PA-MKI WT (Figure 5D; C450A, 92.4 ± 7.8%; WT, 93.8 ± 4.6% of control), while irradiated cells expressing PA-MKI exhibited a ∼70% decrease in phosphorylation (Figure 5D; 30.4 ± 8.1% of control).

Given the role of myosin light chain kinase on peripheral membrane movements,[34] we expressed PA-MKI in COS-7 cells and examined its effects on the protrusive activity of living cells (Figure 6). These cells exhibit a wide variation of protrusion and retraction behaviors, both within a cell and between cells. Not only is MLC phosphorylation modulated in parallel by multiple kinases, these cell morphodynamic behaviors are controlled by a wide-range of other cytoskeleton processes that are independent of myosin activity. Therefore, we expected that acute inhibition of MLCK by PA-MKI might generate subtle effects. Indeed, histograms of local edge velocities (see Methods) in the absence (dark) and presence (light) of activated PA-MKI showed no obvious trends compared to the large spread of the distributions (Figure 6A).

To analyze the morphodynamic behaviors more systematically, we separated protrusion and retraction events and quantified the persistence (duration) and maximal velocity per event. To integrate data from multiple cells we normalized the distributions relative to the median duration and maximal velocities, respectively, during the first dark phase of the

dx.doi.org/10.1021/sb5001356 | ACS Synth. Biol. 2014, 3, 788−795

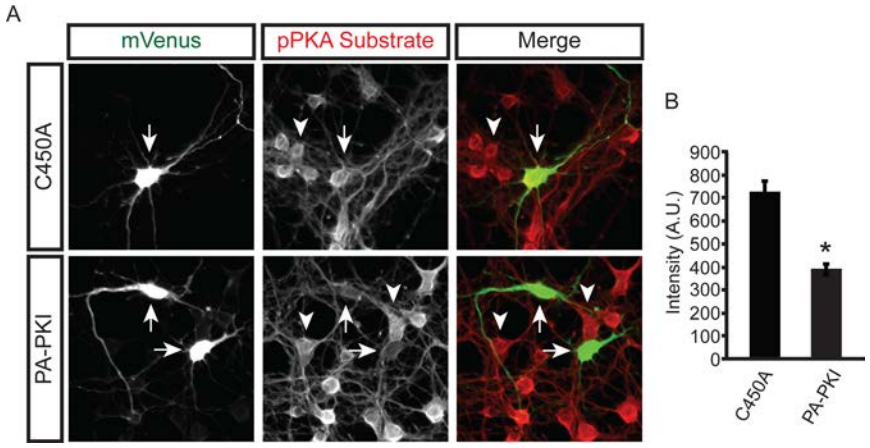

Figure 4. Inhibition of forskolin-induced PKA phosphorylation in primary cultured cortical neurons by PA−PKI. (A) Immunofluorescence of total phosphorylated PKA substrates (pPKA substrate) in cells expressing mVenus−PA-PKI or the dark-state mutant (C450A) of mVenus−PA-PKI. Arrows indicate transfected neurons. Arrowheads indicate untransfected nearby neurons. (B) Fluorescence intensity quantification of (A), $n = 20$ cells per group, $^*p < 0.01$, Student's t test.

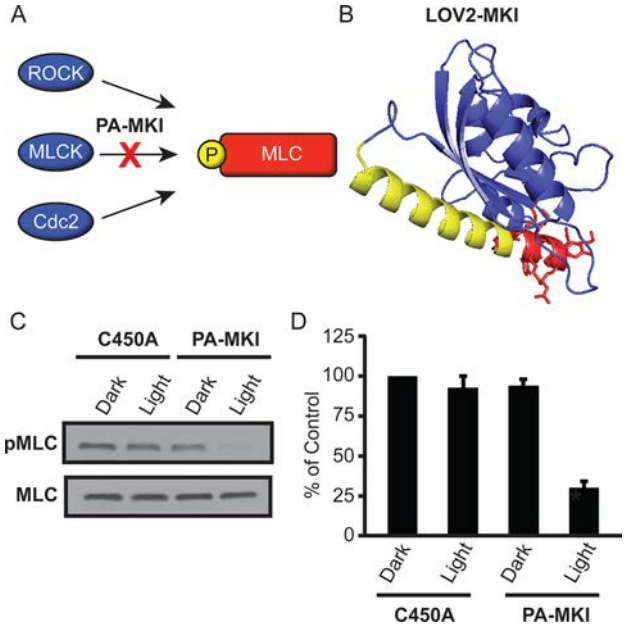

Figure 5. Construction of a photoactivatable myosin light chain kinase inhibitor (PA-MKI). (A) Schematic showing kinases that phosphorylate regulatory myosin light chain. (B) I-TASSER prediction of the conformation for PA-MKI. (C) Western blot showing a reduction of phosphorylated myosin light chain (pMLC) but not total (MLC) in response to blue light irradiation. (D) Quantification of (C), $n = 3$, $^*p < 0.01$, Student's t test.

experiment. Neither median values for the normalized distributions from cells expressing LOV2 alone, nor those expressing PA-MKI showed a statistically significant difference between the dark and light phases (Figure 6D,G). However, the variation between the whisker lengths of the distribution box plots for cells expressing PA-MKI indicated that optical activation of the inhibitor affected the extreme ranges of protrusion velocities. We therefore generated separate distributions of the top (>75%) and bottom (<25%) quartiles (Figure 6B,C,E,F). These analyses revealed that light had no effect on control cells expressing LOV2 alone, but membrane protrusions, and not retractions, were dampened by PA-MKI activation (Figure 6 and Figure S3, Supporting Information). Simply using the membrane permeable MLCK inhibitory peptide 18 produced a dampening of protrusion velocities similar to that of PA-MKI (Figure S4, Supporting Information). These observations are consistent with previous studies showing that myosin light chain kinase plays a role in phosphorylating peripheral myosin light chain to control the structure of actin networks.[34] Moreover, these results demonstrate the utility of photoactivatable peptides in isolating distinct signaling pathways within living cells.

In summary, we report the development of photoswitchable inhibitory peptides that target endogenous kinase signaling. We leveraged the large structural changes that occur during LOV2 irradiation to produce light-responsive kinase inhibitors. Within the field of cell signaling, a great challenge has been to distinguish between competing signaling pathways within a cell. Phosphorylation sites within substrate proteins are often targeted by multiple kinases, and there are currently limited approaches to dissect the biological roles of distinct pathways in cells. Our method provides a minimally invasive approach to address these challenges with high spatiotemporal precision. Peptides are competitive inhibitors of many classes of enzymes and serve a broad range of biological roles, including allosteric modulation[37] and directing the subcellular localization of proteins.[38] Novel classes of peptide therapeutics have been proposed ranging from noncompetitive kinase inhibitors[39] to peptides that regulate angiogenesis,[40] the Rho GTPases,[41] and viral infection.[42,43] The methods described here should be applicable to many other peptides, for investigation and manipulation of processes beyond kinase function.

METHODS

1.1. Antibodies and Reagents. Antiphospho-PKA substrate (RRXS*/T*), antiphospho-CREB (Ser133), anti-CREB, antiphospho-myosin regulatory light chain (Ser19), and antimyosin regulatory light chain were purchased from Cell Signaling Technology. Anti-GFP (JL-8) was purchased from Clontech, anti-β-Actin was purchased from Millipore. Forskolin was purchased from Tocris bioscience. All restriction enzymes were purchased from New England Biolabs. HEK293 cells (ATCC) were cultured in a 5% CO_2 humidified incubator in DMEM, 10% (v/v) fetal bovine serum (Hyclone) and 2 mM Glutamax (Invitrogen). Transfections were performed in 6-well

dx.doi.org/10.1021/sb5001356 | ACS Synth. Biol. 2014, 3, 788−795

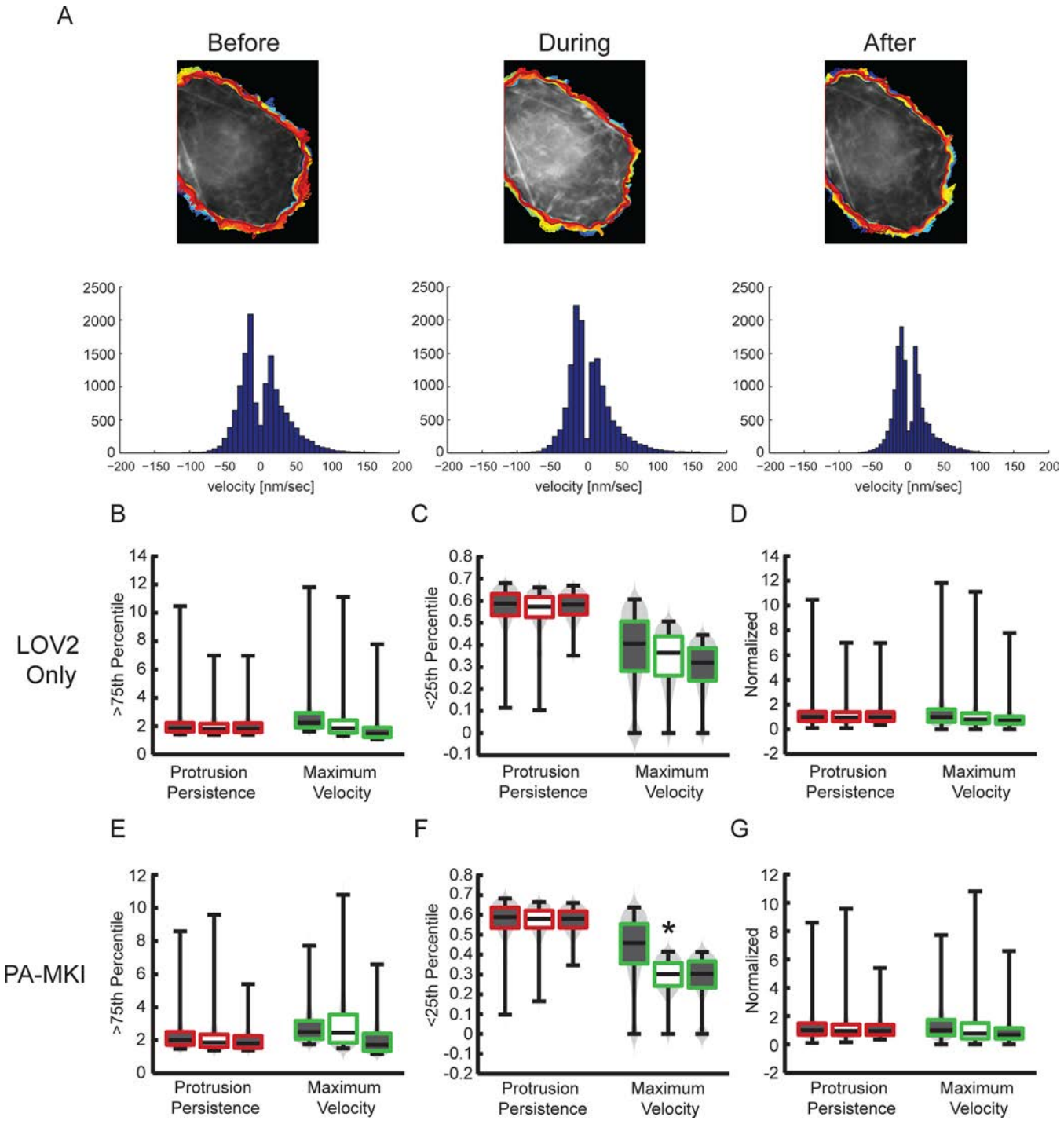

Figure 6. Changes in the protrusion dynamics of COS-7 cells in response to PA-MKI activation. (A) Snapshot of raw image data before (left), during (center), and after (right) light stimulation of a cell expressing PA-MKI. Colors represent the cell edge over the entire imaging interval (blue, early time points; red, late time points). Histograms of instantaneous edge velocity for the three imaging intervals are shown below. (B–D) Box plots showing normalized distributions of protrusion persistence (duration of protrusion phase; red boxes) and maximum velocity per protrusion event (green boxes) for cells expressing LOV2. The three plots represent normalized distributions of the >75th (left), <25th (center), and total (right). Boxes within each plot represent the distributions before (left; gray fill), during (center; white fill), and after (right; gray fill) light stimulation. Data was derived from $n = 6$ cells expressing LOV2 domain only (control). (E–G) Box plots showing normalized distributions of protrusion persistence (duration of protrusion phase; red boxes) and maximum velocity per protrusion event (green boxes) for cells expressing PA-MKI. The three plots represent normalized distributions of the >75th (left), <25th (center), and total (right). Boxes within each plot represent the distributions before (left; gray fill), during (center; white fill), and after (right; gray fill) light stimulation. Data was derived from $n = 6$ cells expressing PA–PKI. Note the decrease in maximum velocity in the <25th percentile of control cells, presumably due to irradiation toxicity. However, in contrast to the decrease in cells expressing PA-MKI, this shift is statistically nonsignificant. *$p < 0.01$, Anderson–Darling test. A detailed description of the analyses can be found in the Methods.

dx.doi.org/10.1021/sb5001356 | *ACS Synth. Biol.* 2014, 3, 788–795

dishes using Lipofectamine 2000 (Invitrogen) according to the manufacturer's instructions.

1.2. Molecular Biology. Inhibitory peptides were fused to the C-terminus of the Jα helix of the LOV domain of *Avena sativa* phototropin 1 (404−541) by polymerase chain reaction and cloned into pmVenus-C1 using XhoI and *Eco*RI sites. Primer sequences used are as follows: LOV2 sense (5′-CTCGAGAAATGGGATCCTTGGCTACTACACTTG-3′), PKI (6−22) antisense (5′-GAATTCCTAAATAGCATT-ACGACGACCAGTACGACCAGAAGCAATAAAATCAGC ATAAGTCTCATCAATATTTTCTGCAGTTTT-3′), PKI (14−22) antisense (5′-GAATTCCTAAATAGCATT-ACGACGACCAGTACGTCCCTCATCAATATTTTCTGC-AGTTTTC-3′), MKI antisense (5′-GAATTCCTATTTA-CGACGATATTTATATTTTTTACGAGAAGCAATAAAA-TCAGCATAAGTCTCATCAATATTTTCTGCAGTTTT-3′).

1.3. Light Irradiation Assay. Cells (HEK293 or neurons) expressing the appropriate constructs were irradiated in an incubator with blue light generated from a 30 W, 30.5 cm × 17 cm panel containing an array of 711 light-emitting diodes (LEDs) radiating 460 nm light (LEDs Super Bright). Cells were irradiated at a distance of 9 cm, which produced a light intensity of 5.6 mW/cm^2. For PKA assays, plates containing transfected cells were placed under the LED array for 15 min prior to the addition of forskolin. Plates were placed back into the incubator and irradiated for an additional 1.5 h. For MLCK assays, cells were irradiated in the incubator for 1−1.5 h. Cells were lysed in NuPage LDS sample buffer (Life Technologies) supplemented with 1% β-mercaptoethanol, 1× Complete Mini protease inhibitor cocktail (Roche), and 1× Halt Phosphatase Inhibitor Cocktail (Thermo Scientific).

1.4. Dissociated Neuron Cultures. Mouse cortices were dissected from embryonic day (E) 13.5 to E 16.5 animals, trypsinized with TrypLE express at 37°C for 10 min, and dissociated with a fire-polished Pasteur pipet in plating medium (Neurobasal medium with 5% fetal bovine serum, Glutamax, B27 (Invitrogen), and Antibiotic-Antimycotic (Invitrogen)). Dissociated neurons were seeded onto 24-well plates containing coverslips coated with poly-D-lysine (0.1 mg/mL) at a density of 1 × 10^5 cells/well. Neurons were incubated at 37 °C with 5% CO_2 and the plating medium changed into Neurobasal medium supplemented with 4.84 mg/mL Uridine 5′-triphosphate (Sigma), 2.46 mg/mL 5-fluoro 2-deoxyuridine (Sigma), Glutamax, B27, and Antibiotic-Antimycotic at days *in vitro* (DIV) 3 and DIV 6. Neurons were transfected on DIV 6 with various DNA constructs using Lipofectamine 2000. After 48 h in culture, neurons were irradiated upon PKA induction with forskolin and fixed with 4% paraformaldehyde (PFA)/4% sucrose in phosphate buffered saline for 30 min.

1.5. Immunohistochemistry. Freshly fixed neurons were washed with PBS and permeabilized and blocked with 8% bovine serum albumin (BSA) in PBS containing 0.1% Triton X-100. Neurons were then incubated with primary antibodies at 4 °C overnight. After washing with PBS, appropriate Alexa Fluor-conjugated secondary antibodies (Life Technologies) were used to detect the signal. The secondary antibody was incubated at room temperature for 1 h. Coverslips were mounted onto glass slides using Fluoro-Gel mounting medium (Electron Microscopy Sciences). To quantify PKA activity in neurons, Metamorph software (Molecular Devices) was used to create a binary mask of the cells from the mVenus images. This defined the area of the transfected cell of interest. The average intensity of the immunofluorescence signal produced from staining with the antiphospho-PKA substrate antibody was measured within this defined region.

1.6. Live Cell Imaging. COS-7 cells were transiently cotransfected with LifeAct-mCherry 20−28 h before imaging. Cells used for live cell imaging were seeded on coverslips coated with 10 mg/mL fibronectin in Ham's F-12K medium free of Phenol Red and containing 5% FBS. Coverslips were mounted in an Attofluor live cell chamber (Invitrogen) placed on a heated microscope stage (Warner). Images were acquired using an Olympus IX81-ZDC microscope equipped with a CoolSNAP HQ2 14-bit camera (Photometrics). Bandpass and neutral density filters (Chroma) were switched using motorized filter wheels (Ludl Electronic Products) controlled by Metamorph Software version 7.6.4. YFP and mCherry images were acquired using a 100 W Hg arc lamp with a 1% ND filter, and 510−520 nm or 565−595 nm band-pass filters respectively, for 500 ms. For peptide activation, a 5% ND filter and a 426−446 nm band-pass filter were used. The activation period of imaging consisted of a pulse protocol (alternating 5 s light 5 s dark) that lasted a total of 15 min. Images were processed post acquisition *via* shading correction, background subtraction, and binary masking using Metamorph software (Molecular Devices).

1.7. Image Analysis. The images acquired by live-cell microscopy were analyzed using in-house software. For each frame of the movie, the cell edge was first detected and then divided into a series of 1 μm^2 wide segments, as described in.[44] Local cell edge velocities were calculated by tracking the displacement of segments from one frame to the next. Per-segment velocity time series were then divided into protrusion and retraction events, and for each event the duration and maximal velocity recorded. In order to quantify changes in these parameters between the initial basal (dark), stimulated (light), and recovery (dark) imaging intervals, the distributions were normalized by the median value of the basal interval. This normalization corrected for distribution bias associated with the heterogeneity of morphodynamic behavior among cells. Both persistence and max protrusion/retraction velocities approximately followed a log-normal distribution. The Anderson−Darling Test was used on the exponentiated values to determine the significance of observed differences among the distributions collected from the three imaging intervals.

■ ASSOCIATED CONTENT

Supporting Information

Supporting methods and Figures S1−S4. This material is available free of charge *via* the Internet at http://pubs.acs.org.

■ AUTHOR INFORMATION

Corresponding Author

*E-mail: khahn@med.unc.edu.

Author Contributions

#J. J. Yi and H. Wang contributed equally to this work.

Notes

The authors declare no competing financial interest.

■ ACKNOWLEDGMENTS

We are grateful to the NIH for funding this work (R01 GM 090317, R01 GM 102924, and P01-GM103723). J.J.Y. is a recipient of the Christina Castellana Postdoctoral Fellowship from the Foundation for Angelman Syndrome Therapeutics.

H.W. is a recipient of an Arthritis Foundation Postdoctoral Fellowship. M.V. is a recipient of an NIH F32 fellowship (5F32GM103278−02). We are grateful to Marie Rougie, Evan Trudeau, and Betsy Clarke for expert technical and administrative support. We are grateful to Jaya Miriyala for preparing primary neuronal cultures.

REFERENCES

(1) Lahiry, P., Torkamani, A., Schork, N. J., and Hegele, R. A. (2010) Kinase mutations in human disease: interpreting genotype-phenotype relationships. *Nat. Rev. Genet. 11*, 60−74.

(2) Manning, G., Plowman, G. D., Hunter, T., and Sudarsanam, S. (2002) Evolution of protein kinase signaling from yeast to man. *Trends Biochem. Sci. 27*, 514−520.

(3) Manning, B. D., and Cantley, L. C. (2002) Hitting the target: emerging technologies in the search for kinase substrates. *Sci. Signaling 2002*, pe49.

(4) Yin, T., and Wu, Y. I. (2013) Guiding lights: recent developments in optogenetic control of biochemical signals. *Pfluegers Arch. 465*, 397−408.

(5) Lungu, O. I., Hallett, R. A., Choi, E. J., Aiken, M. J., Hahn, K. M., and Kuhlman, B. (2012) Designing photoswitchable peptides using the AsLOV2 domain. *Chem. Biol. 19*, 507−517.

(6) Strickland, D., Lin, Y., Wagner, E., Hope, C. M., Zayner, J., Antoniou, C., Sosnick, T. R., Weiss, E. L., and Glotzer, M. (2012) TULIPs: tunable, light-controlled interacting protein tags for cell biology. *Nat. Methods 9*, 379−384.

(7) Crosson, S., and Moffat, K. (2001) Structure of a flavin-binding plant photoreceptor domain: insights into light-mediated signal transduction. *Proc. Natl. Acad. Sci. U. S. A. 98*, 2995−3000.

(8) Halavaty, A. S., and Moffat, K. (2007) N- and C-terminal flanking regions modulate light-induced signal transduction in the LOV2 domain of the blue light sensor phototropin 1 from *Avena sativa*. *Biochemistry 46*, 14001−14009.

(9) Harper, S. M., Neil, L. C., and Gardner, K. H. (2003) Structural basis of a phototropin light switch. *Science 301*, 1541−1544.

(10) Harper, S. M., Christie, J. M., and Gardner, K. H. (2004) Disruption of the LOV-Jalpha helix interaction activates phototropin kinase activity. *Biochemistry 43*, 16184−16192.

(11) Swartz, T. E., Corchnoy, S. B., Christie, J. M., Lewis, J. W., Szundi, I., Briggs, W. R., and Bogomolni, R. A. (2001) The photocycle of a flavin-binding domain of the blue light photoreceptor phototropin. *J. Biol. Chem. 276*, 36493−36500.

(12) Swartz, T. E., Wenzel, P. J., Corchnoy, S. B., Briggs, W. R., and Bogomolni, R. A. (2002) Vibration spectroscopy reveals light-induced chromophore and protein structural changes in the LOV2 domain of the plant blue-light receptor phototropin 1. *Biochemistry 41*, 7183−7189.

(13) Zoltowski, B. D., Vaccaro, B., and Crane, B. R. (2009) Mechanism-based tuning of a LOV domain photoreceptor. *Nat. Chem. Biol. 5*, 827−834.

(14) Walsh, D. A., Ashby, C. D., Gonzalez, C., Calkins, D., and Fischer, E. H. (1971) Krebs EG: Purification and characterization of a protein inhibitor of adenosine 3′,5′-monophosphate-dependent protein kinases. *J. Biol. Chem. 246*, 1977−1985.

(15) Lu, Y., Zha, X. M., Kim, E. Y., Schachtele, S., Dailey, M. E., Hall, D. D., Strack, S., Green, S. H., Hoffman, D. A., and Hell, J. W. (2011) A kinase anchor protein 150 (AKAP150)-associated protein kinase A limits dendritic spine density. *J. Biol. Chem. 286*, 26496−26506.

(16) Tkachenko, E., Sabouri-Ghomi, M., Pertz, O., Kim, C., Gutierrez, E., Machacek, M., Groisman, A., Danuser, G., and Ginsberg, M. H. (2011) Protein kinase A governs a RhoA-RhoGDI protrusion-retraction pacemaker in migrating cells. *Nat. Cell Biol. 13*, 660−667.

(17) Salomon, M., Christie, J. M., Knieb, E., Lempert, U., and Briggs, W. R. (2000) Photochemical and mutational analysis of the FMN-binding domains of the plant blue light receptor, phototropin. *Biochemistry 39*, 9401−9410.

(18) Pearson, R. B., and Kemp, B. E. (1991) Protein kinase phosphorylation site sequences and consensus specificity motifs: tabulations. *Methods Enzymol. 200*, 62−81.

(19) Wu, Y. I., Frey, D., Lungu, O. I., Jaehrig, A., Schlichting, I., Kuhlman, B., and Hahn, K. M. (2009) A genetically encoded photoactivatable Rac controls the motility of living cells. *Nature 461*, 104−108.

(20) Stofega, M., DerMardirossian, C., and Bokoch, G. M. (2006) Affinity-based assay of Rho guanosine triphosphatase activation. *Methods Mol. Biol. 332*, 269−279.

(21) Wu, S., Skolnick, J., and Zhang, Y. (2007) *Ab initio* modeling of small proteins by iterative TASSER simulations. *BMC Biol. 5*, 17.

(22) Zhang, Y. (2008) I-TASSER server for protein 3D structure prediction. *BMC Bioinf. 9*, 40.

(23) Montminy, M. (1997) Transcriptional regulation by cyclic AMP. *Annu. Rev. Biochem. 66*, 807−822.

(24) Xie, H., and Rothstein, T. L. (1995) Protein kinase C mediates activation of nuclear cAMP response element-binding protein (CREB) in B lymphocytes stimulated through surface Ig. *J. Immunol. 154*, 1717−1723.

(25) Matthews, R. P., Guthrie, C. R., Wailes, L. M., Zhao, X., Means, A. R., and McKnight, G. S. (1994) Calcium/calmodulin-dependent protein kinase types II and IV differentially regulate CREB-dependent gene expression. *Mol. Cell. Biol. 14*, 6107−6116.

(26) Bohm, M., Moellmann, G., Cheng, E., Alvarez-Franco, M., Wagner, S., Sassone-Corsi, P., and Halaban, R. (1995) Identification of p90RSK as the probable CREB-Ser133 kinase in human melanocytes. *Cell Growth Differ. 6*, 291−302.

(27) Arthur, J. S., and Cohen, P. (2000) MSK1 is required for CREB phosphorylation in response to mitogens in mouse embryonic stem cells. *FEBS Lett. 482*, 44−48.

(28) Tan, Y., Rouse, J., Zhang, A., Cariati, S., Cohen, P., and Comb, M. J. (1996) FGF and stress regulate CREB and ATF-1 *via* a pathway involving p38 MAP kinase and MAPKAP kinase-2. *EMBO J. 15*, 4629−4642.

(29) Carruthers, A. M., Sellers, L. A., Jenkins, D. W., Jarvie, E. M., Feniuk, W., and Humphrey, P. P. (2001) Adenosine A(1) receptor-mediated inhibition of protein kinase A-induced calcitonin gene-related peptide release from rat trigeminal neurons. *Mol. Pharmacol. 59*, 1533−1541.

(30) Inglefield, J. R., Mundy, W. R., Meacham, C. A., and Shafer, T. J. (2002) Identification of calcium-dependent and -independent signaling pathways involved in polychlorinated biphenyl-induced cyclic AMP-responsive element-binding protein phosphorylation in developing cortical neurons. *Neuroscience 115*, 559−573.

(31) Namkoong, S., Kim, C. K., Cho, Y. L., Kim, J. H., Lee, H., Ha, K. S., Choe, J., Kim, P. H., Won, M. H., Kwon, Y. G., Shim, E. B., and Kim, Y. M. (2009) Forskolin increases angiogenesis through the coordinated cross-talk of PKA-dependent VEGF expression and Epac-mediated PI3K/Akt/eNOS signaling. *Cell. Signalling 21*, 906−915.

(32) Yang, D. C., Tsay, H. J., Lin, S. Y., Chiou, S. H., Li, M. J., Chang, T. J., and Hung, S. C. (2008) cAMP/PKA regulates osteogenesis, adipogenesis and ratio of RANKL/OPG mRNA expression in mesenchymal stem cells by suppressing leptin. *PLoS One 3*, e1540.

(33) Lukas, T. J., Mirzoeva, S., Slomczynska, U., and Watterson, D. M. (1999) Identification of novel classes of protein kinase inhibitors using combinatorial peptide chemistry based on functional genomics knowledge. *J. Med. Chem. 42*, 910−919.

(34) Ikebe, M., and Hartshorne, D. J. (1985) Phosphorylation of smooth muscle myosin at two distinct sites by myosin light chain kinase. *J. Biol. Chem. 260*, 10027−10031.

(35) Amano, M., Ito, M., Kimura, K., Fukata, Y., Chihara, K., Nakano, T., Matsuura, Y., and Kaibuchi, K. (1996) Phosphorylation and activation of myosin by Rho-associated kinase (Rho-kinase). *J. Biol. Chem. 271*, 20246−20249.

(36) Satterwhite, L. L., Lohka, M. J., Wilson, K. L., Scherson, T. Y., Cisek, L. J., Corden, J. L., and Pollard, T. D. (1992) Phosphorylation of myosin-II regulatory light chain by cyclin-p34cdc2: a mechanism for the timing of cytokinesis. *J. Cell Biol. 118*, 595−605.

(37) Lockless, S. W., and Ranganathan, R. (1999) Evolutionarily conserved pathways of energetic connectivity in protein families. *Science 286*, 295−299.
(38) Conti, E., Uy, M., Leighton, L., Blobel, G., and Kuriyan, J. (1998) Crystallographic analysis of the recognition of a nuclear localization signal by the nuclear import factor karyopherin alpha. *Cell 94*, 193−204.
(39) Eldar-Finkelman, H., and Eisenstein, M. (2009) Peptide inhibitors targeting protein kinases. *Curr. Pharm. Des. 15*, 2463−2470.
(40) D'Andrea, L. D., Del Gatto, A., De Rosa, L., Romanelli, A., and Pedone, C. (2009) Peptides targeting angiogenesis related growth factor receptors. *Curr. Pharm. Des. 15*, 2414−2429.
(41) Marchioni, F., and Zheng, Y. (2009) Targeting rho GTPases by peptidic structures. *Curr. Pharm. Des. 15*, 2481−2487.
(42) Andreola, M. L. (2009) Therapeutic potential of peptide motifs against HIV-1 reverse transcriptase and integrase. *Curr. Pharm. Des. 15*, 2508−2519.
(43) Kashanchi, F., and Kehn-Hall, K. (2009) Cyclin dependent kinases as attractive targets to prevent transcription from viral genomes. *Curr. Pharm. Des. 15*, 2520−2532.
(44) Machacek, M., and Danuser, G. (2006) Morphodynamic profiling of protrusion phenotypes. *Biophys. J. 90*, 1439−1452.